Diversity Framed Slotted Aloha with Interference Cancellation for Maritime Satellite Communications

Manlio Bacco*, Pietro Cassará*, Alberto Gotta*, Tomaso de Cola†

*CNR, Institute of Information Science and Technologies, Pisa, Italy
†DLR, Institute of Communications and Navigation, Oberpfaffenhofen, Germany

***Abstract*—Providing reliable and efficient connectivity for maritime systems is a key objective to enable new services and to offer anytime-anywhere communication solutions to vessels operating in remote areas (e.g. oceans). Such a task has recently become quite compelling because of the increasing maritime traffic, which should be supported by an information distribution infrastructure in order to guarantee efficient data communication among vessels and control centres on land. To this end, satellites are the perfect candidates for achieving such an objective.**

This paper focuses on the case of messaging from moving vessels to fixed control centres on land by means of advanced channel random access schemes exploiting time diversity. In more detail, the paper extends an existing theoretical framework to evaluate the packet loss probability in Framed Slotted ALOHA systems by delving into the probability distribution of both colliding users within a frame and their replicas in time slots. The theoretical framework is validated through simulations campaigns, showing a good match between analytical and simulated results.

***Index Terms*—Maritime SatCom, M2M, D-FSA, Interference Cancellation, Random Access.**

I. Introduction

According to recent forecasts, the maritime traffic is expected to dramatically increase by at least 50% in terms of vessel calls at main harbour for what concerns cargo arrival and departures. If we also consider the contribution given by ships in the leisure segments (e.g., cruises), the overall maritime traffic will see a considerable number of ships per day over seas. This aspect has an importance reflection into the ever increasing demand of connectivity coming from cruise passengers and general purpose messaging from all vessels. As a result, the necessity of an anywhere-anytime communication paradigm, capable of serving as many users as possible, and offering them the desired quality of service is calling for novel and more sophisticated telecommunication concepts.

From this standpoint, satellite communication is the most appealing technology solution to offer connectivity because of the intrinsic broadcast/multicast transmission capabilities as well as the very wide geographical coverage. On the one hand, the increasing demand for multimedia content from leisure travel passengers will be satisfied by the large-capacity forward link of next generation satellite systems (e.g., High Throughput Satellite). On the other hand, services such as fleet management, telemetry, and in general maritime Internet of Things (IoT) applications (e.g., surveillance and detection), will certainly benefit from ubiquitous satellite connectivity with limited bandwidth requirements.

A central role for the satellite communication success in the maritime domain is played by the medium contention schemes. If, on the one hand, historically satellite systems have been implementing dedicated access schemes (e.g., TDMA-like), a recent trend is to also provide random access (RA) schemes for severely reducing the channel access delay that could otherwise penalize IoT service performance. In particular, random access ALOHA schemes have regained popularity in the last fifteen years in the context of satellite communications and turned out to be particularly attractive for the support of IoT services in maritime domains. To this regard, the scientific community has elaborated several schemes in the last years [1], [2], by taking the consolidated Slotted Aloha (SA) and Frame Slotted Aloha (FSA) schemes as baseline and extending them with novel concepts such as time diversity (e.g, in Diversity Frame Slotted Aloha, D-FSA [3]) and Interference Cancellation (IC), the latter being exploited in many proposals such as CRDSA [4], IRSA [5], and CSA [6]. In more detail, FSA and D-FSA schemes may introduce significant number of packet losses or even cause undesirable service unavailability. On the other hand, a great performance improvement, in terms of throughput, comes from applying Successive IC (SIC) to D-FSA. In this case, the replicas transmitted within a Medium Access Control (MAC) frame keep a pointer to the twin slots: whenever a clean burst is detected and successfully decoded, the potential interference contribution caused by the twin replica is cancelled in the pointed slot, hence resulting in a remarkable throughput improvement with respect to SA. A further improvement may be achieved either by increasing the number of replicas to K, either letting K be a random variable sorted by a discrete distribution [5], or being K the coded fragments of a packet of m bits, with $m < K \cdot b$, and b being the size [bits] of a time slot [6].

In spite of the large literature addressing RA schemes for satellite systems, only few studies actually considered the case of a known number of machine-to-machine (M2M) terminals [7] and none of them provides a complete statistical characterization of the system. In fact, when an RA system undergoes a variable traffic load (as for instance with sporadic and unpredictable M2M traffic), so that the system cannot be considered in steady state, then first- and second-order statistics are not sufficient to characterize the performance of the system. On the contrary, knowledge of the probability distribution of the number of collided users would help in carrying out a more thorough performance analysis, which is an important scientific problem not completely solved by the literature, to the best of the authors' knowledge.

To this aim, this paper elaborates an analytical framework to calculate both the distribution of the number colliding users and the average number of colliding packets per time slot in each frame of a D-FSA satellite-based system. Eventually, the conducted validations campaigns by means of simulations have shown a good match between the framework and the simulations in the case of maritime communications. Moreover, the collected performance results have also helped in shedding some light about some aspects of RA-based satellite schemes under variable load traffic that other works could not thoroughly analyse.

The remainder of this paper is structured as follows. The system model and the theoretical framework are described in Sections II and III, respectively. Validation of the theoretical findings through simulation campaigns is in Section IV, whereas final conclusions and considerations about future works are drawn in Section V.

II. System Overview

A. Reference Scenario

This paper focuses on supporting geostationary (GEO) satellite systems for data communications, established between remote vessels operating on sea (i.e., far from harbours), and processing and control centers positioned on land (i.e, in proximity of harbours). Typically, this application scenario has seen the use of Low Earth Orbit (LEO) satellite constellations (i.e., Orbcomm), because of the limited capacity demand, coming from the moderate number of vessels in the past, and the inherent lower latency characterizing LEO systems with respect to the GEO counterpart.

More recently, however, GEO systems supporting maritime communications have become quite attractive, because of the larger data traffic being injected into satellite systems, as a consequence of the increase of traffic over oceans. Moreover, some of the main GEO satellite operators have extended their business towards satellite-on-the move systems, hence naturally embracing additional maritime data services. This is for instance the case of Inmarsat satellite fleet, which is also taken as technology reference throughout the rest of this work. In more words, this system provides many types of commercial communication services based on both L-band (1-2 GHz) and Ka-band (26-40 GHz) technologies. By means of the L-band technology, low speeds communication services can be provided with a high level of reliability; the Ka-band is instead mostly used for high speeds throughput communication services, as demanded by real-time applications.

The main focus of this paper is on the Ka frequency band, so as to enable highly reliable and timely M2M services, in terms of monitoring and control of vessel activities. As such, this communication system is well suited to provide coverage over a large area with users in mobility whilst guaranteeing the needed data rate for the real-time communication of diverse sensors and actuators displaced on vessels.

B. Channel Model

The characterization of the maritime satellite channel has been largely investigated [8]–[10] in the past decades. Based on the conducted measurement campaigns and the corresponding channel models, we assume in this work that the envelope of the signal received by the mobile terminal follows the Rice distribution, which describes the terminal-satellite communications in line of sight (LoS), to which additional distorted signal replicas are summed up to account for signal reflection caused by the water surface. In more detail, the Rice factor characterizing the received power distribution of probability depends on the elevation angle: by taking into account that the received power due to LoS communication increases with the elevation angle, the Rice factor increases as well. The delay incurred between the reception of the LoS path signal and the multi-path components falls within hundreds of nanoseconds. On the other hand, the impulse channel response exhibits a number of echoes that can be assumed as Poisson-distributed with rate between 1 and 2, as in the case of open space communications, hence indicating a rapid decay of the impulse channel response.

III. Theoretical Framework

A. Loop Model

Let us introduce the fundamental loop concept, which we use in what follows to characterize both D-FSA and the contention resolution in all the recent RA variants with IC. A *loop* occurs when two or more users send their replicas in the same time slot(s).

An l-order loop is given by $l+1$ users with $l \geq 1$, i.e. $l+1$ users[1] have chosen exactly the same pool $\mathcal{L}$ of time slots to send their replicas. Therefore, all the time slots $t_i \in \mathcal{L}$ are affected by a collision, which means at least two users among the $l+1$ ones transmit in that time slot. This is shown by means of an example in Table I: the symbol *x* represents a replica of the users u_1 , u_2 , u_3 belonging to the loop, and its pool of time slots $\mathcal{L}$ is $\{t_1 , t_2 , t_5 , t_6\}$. Instead, the symbol *o* in Table I represents the replicas transmitted by users non in loop, i.e., with at least a replica in a time slot with no other packets, as in ($u_4 \rightarrow t_3$, $u_5 \rightarrow t_4$). Note that, the users u_1 , u_2 , u_3 are in loop regardless of other users. Loops cause a contention between users that can be very hard to be decoded, unless other mechanisms are in place, i.e. when coding techniques

TABLE I: Example of the pool of time slots involved in a loop with $l = 2$ users.

	t_1	t_2	t_3	t_4	t_5	t_6
u_1	x				x	x
u_2	x	x			x	
u_3	x	x				x
u_4	o		o		o	
u_5	o			o		o

[1]The case $l = 0$ means that there is no loop.

are applied or when power imbalance between users occurs, thus giving rise to the *capture effect*. Loops between two users can only occur if they both have replicas in the same exact time slots. Otherwise, loops between more than two users can occur in different ways, so that counting them can prove challenging. The probability of having loops in a simple case, in which all the collided users share exactly the same time slots, has been investigated in [11]. Loops are one of the main reasons for packet losses, measured by means of the packet loss ratio (PLR). In D-FSA, each user selects a set of K distinct time slots from N in a MAC frame. Then, the user can choose any of the possible combinations with an equal probability $q = \binom{N}{K}^{-1}$. Consider now a generic packet of interest (PoI). The probability p_l that the sender of the PoI is in a loop with l users follows a binomial distribution, as shown in [11]:

$$p_l(U, q) = \binom{U-1}{l} \cdot q^l \cdot (1-q)^{U-1-l} \tag{1}$$

where U is the number of users per frame. It can be easily verified that p_l is negligible for $N = 100$, $k = 3$, and $U \to N$ for any $l > 1$. In fact, this would require that all the $l+1$ users must select exactly the same K-tuple.

Actually, PLR tend to 1 when $U \geq N$ [12], i.e., when the number of users is equal or greater than the number of available time slots per frame. Therefore, Equation (1) does not accurately model the statistical occurrence of loops in D-FSA systems.

B. Contention Resolution and Interference Cancellation

We recall that $\Gamma(x)$, as characterized in [11], [13], is a polynomial interpolation that provides the packet error rate curve for a given channel code and modulation scheme as a function of the argument x, which represents the E_b/N_0 value [dB]. The probability $(1 - \zeta_l)$ that a packet in a loop with l other interfering packets can be correctly decoded, under the hypothesis of AWGN channel and perfect power balancing among all users, is defined in [11], [13], and ζ_l can be expressed as:

$$\zeta_l = \Gamma^K \left(10\, log_{10} \left[\frac{E_b/N_0}{1 + E_b/N_0\, l} \, \frac{1}{r\, log_2\, M} \right] \right), \tag{2}$$

with coding rate r, and M symbols. By relaxing the condition on the perfect power balancing among users, the interfering contribution at the denominator in Eq. (2) must be substituted by $\sum_{i=1}^{l}(E_b/N_0)_i$. The SIC process aims at reducing the degree l of a loop by iteratively performing cancellation of packets correctly decoded in other time slots. Yet, in the case of spread spectrum techniques, $E_b/N_0\, l$ in Eq. (2) must be substituted by $(E_b/N_0)/S_f\, l$ as shown in [13], where S_f is the spreading factor.

From Eqs. (1) and (2), it follows that the probability that a PoI remains in a loop of degree l with $l = 1, 2, \cdots, U-1$ users (after SIC) is given in [11], [13] as:

$$PLR = \sum_{l=1}^{U-1} \left[p_l + \sum_{n=l+1}^{U-1} p'_n \binom{n}{n-l} \zeta_n^l \cdot (1-\zeta_n)^{n-l} \right] \zeta_l^{l+1}. \tag{3}$$

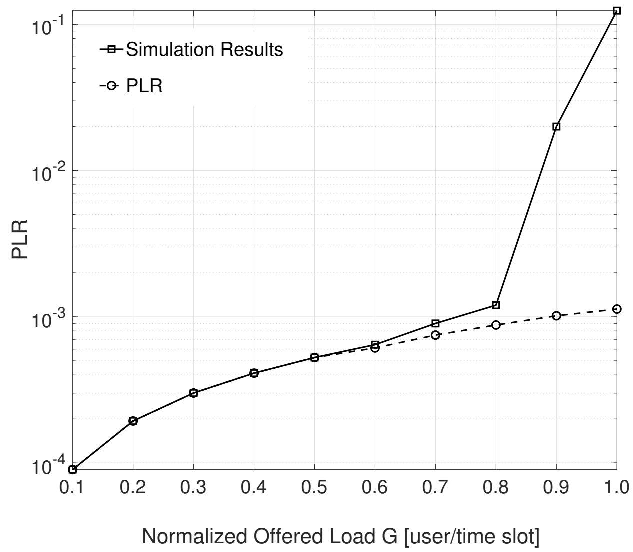

Fig. 1: Simulated and analytical results as in [13] for 2-CRDSA, $[E_s/N_0]$ = 10 dB, K = 2, U = 100, IC iterations $\leq$ 15, r = 1/3, 3GPP FEC with block size b = 100 bits, QPSK modulation with $M = 4$.

The term inside the square bracket is the probability of having a loop of degree l, starting from the initial probability p_l plus the probability that some of the higher order loops can be downgraded to loops of order l, thanks to SIC. The term outside of the square bracket represents the probability that none of the packets in the loop of order l can be decoded.

It is worth noting that the number of interfering packets with a PoI is *not* always equal to l (see Eq. (2)) if $l+1$ users are in loop. In fact, this is true only when two users are in loop ($l = 1$) and transmit into the same K-tuple of time slots.

For $l > 1$, the set of time slots of the users in loop ranges from a minimum of K time slots (as in Eq. (2)) up to $\lfloor (l+1)K/2 \rfloor$; hence, the number of packets i interfering with a given PoI in a time slot is a *r.v.*, which can assume values $1 \cdots l$ with probability $P_I(i \,|\, l)$, as shown in Table I.

Therefore, the term l in Eq. (2) can be substituted by the approximation $E[I \,|\, l]$, which is defined as:

$$E[I \,|\, l] = \sum_{j=1}^{l} j \cdot P_I(j \,|\, l). \tag{4}$$

Actually, l should be substituted with i, and Eq. (2) should be weighted over $P_I(i \,|\, l)$, as follows:

$$\zeta_l = \sum_{j=1}^{l} \Gamma^K \left(10\, log_{10} \left[\frac{E_b/N_0}{1 + E_b/N_0\, j} \frac{1}{r\, log_2 M} \right] \right) P_I(j \,|\, l). \tag{5}$$

Figure 1 depicts the comparison between the analytical model in Eq. (3) and the simulations based on the use of 2-CRDSA, as proposed in [13]. The simulations show that the analytical model underestimates PLR for normalized loads higher than 0.6, according to the findings at the end of Section III-A. We recall that 2-CRDSA provides a p_l with small divergence from the empirical curve; if considering

$K > 2$, the phenomenon is more evident since the number of possible combinations of K-tuples grows rapidly with K and U. Anyway, 3-CRDSA provides better performance in terms of throughput w.r.t. 2-CRDSA or IRSA [14]. Moreover, if congestion control algorithms are operated by the upper layer protocols (i.e, transport layer), it turns out that the working points are subject to PLR close to 10^{-3} and to 10^{-2}, for TCP [15] and TFRC-like [16] respectively, when 3-CRDSA is in use. Thus, according to Figure 1 and to its simulation parameters, the average load G might go up to 0.8-0.9 bit/symbols of gross application layer traffic, with an approximation error of one or two decades. This fosters further investigations mainly on two statistics: (*i*) the distribution of the number of users in a loop occurred in a frame; (*ii*) the distribution of the number of time slots involved in a loop or, dually, the average number of packets interfering with a PoI.

C. Multi User Interference

We recall that we assume a communication being affected by Rice fading, in order to consider a realistic condition that embraces a LoS with possible multipath fading as usually occurring in satellite maritime communications. Without loss of generality, we further assume that the spatial distribution of concurrently transmitting users follows a deterministic general model, i.e., a finite number of users are within a finite region and they transmit with the same level of E_b/N_0 [dB]. Under these assumptions, we provide a solution for the Probability Density Function (PDF) of the interference generated by a set of $l+1$ user by exploiting Palm's theory and, in particular, the conditional probability generating functional [17], [18]. The interference generated by $l+1$ users in a time slot is:

$$I_{l+1} = \sum_{j=1}^{l+1} \mathcal{B}_j\left(U, \frac{K}{N}\right)\left(\frac{E_b}{N_0}\right)_j, \qquad (6)$$

where $\mathcal{B}_j\left(U, \frac{K}{N}\right)$ is the probability of having a subset $l+1$ out of U active users transmitting in a time slot, according to a binomial distribution:

$$\mathcal{B}_j\left(U, \frac{K}{N}\right) = \binom{U}{j}\left(\frac{K}{N}\right)^j\left(1-\frac{K}{N}\right)^{U-j}. \qquad (7)$$

The term $\left(\frac{E_b}{N_0}\right)_j$ is user j's SNR.

The evaluation of the interference I_{l+1} can be obtained through the numerical inversion of its probability generating functional, defined as:

$$\mathcal{L}_{I_{l+1}}(s) = \mathbb{E}[exp^{(-s\, I_{l+1})}], \qquad (8)$$

which is needed to evaluate E_b/N_0 in Eq. (2).

Figure 2 shows a sample of the PDF of the SNIR ψ at the receiver, given the number i of interfering packets with the PoI, for a load $G = 0.5$ (i.e., 32 users experiencing Rician fading and transmitting in a frame composed of 64 time slots). The plotted areas represent the empirical distributions, while the dotted lines with markers are the relative analytical

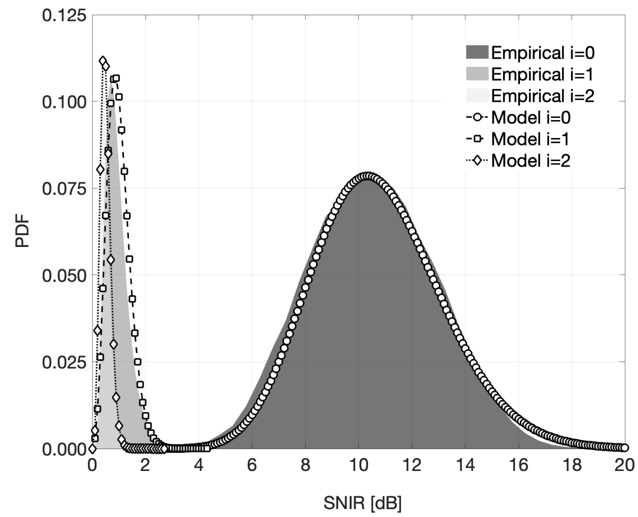

Fig. 2: Example of empirical PDF vs. SNIR model ($G = 0.5$, $i = \{0, 1, 2\}$).

curves $P_\Psi(\psi \,|\, i)$ derived by numerically solving Eq. (8). Using $P_\Psi(\psi \,|\, i)$, equation (5) can be generally written as:

$$\hat{\zeta}_l = \sum_{j=1}^{l} \Gamma^K(E[\psi \,|\, j])\; P_I(j \,|\, l), \qquad (9)$$

where $E[\psi \,|\, j] = \int \psi\, P_\Psi(\psi \,|\, j)\, d\psi$.

Figure 2 shows the cases in which the interfering packets $i = \{0, 1, 2\}$. In fact, if $i > 2$, a packet could be decoded either thanks to a spreading factor $S_f > 1$ (this is not the case of this paper), or through SIC with contention resolution, as addressed in this paper and further discussed in Section III-B.

IV. Performance Evaluation

The performance evaluation thereafter described has been obtained through extensive simulation campaigns, based on the use of the S-NS3 simulator [19]. Further development allows to also account for the multipath fading channel model in order to properly characterise a satellite maritime channel. We assume a number of replicas $K = 3$ over a frame of $N = 64$ time slots. By using the measurements of the direct-to-multipath signal power ratio versus satellite elevation provided in [8], [9] for the Inmarsat system, a Rice-factor of 14.5 dB can be obtained for an average elevation angle $\theta = 19°$. The corresponding delay power profile of the simulated channel exhibits an RMS delay spread $\tau = 49$ ns and a coherence bandwidth of $B_c = 3.2$ MHz, the latter computed according to $B_c = \frac{1}{2\pi\tau}$. The channel coherence time can be approximated as $T_c \approx 1/(f_c \frac{v\, cos(\theta)}{c})$, yielding $T_c = 2.6$ ms for a carrier frequency $f_c = 29.5$ GHz and an average speed of the mobile terminal $v = 15$ Km/h, as then used in our simulations. Figure 3 shows the empirical Probability Mass Functions (PMFs) $\hat{p}_l$ of the number of users interfering with a PoI for different values of G in a significant range compared to the distribution p_l in Eq. (1) for $l = 1 \cdots 63$. For G in the range $0.5 - 0.6$, Eq. (1) shows a discrete approximation of the empirical distribution of the interfering users. Clearly,

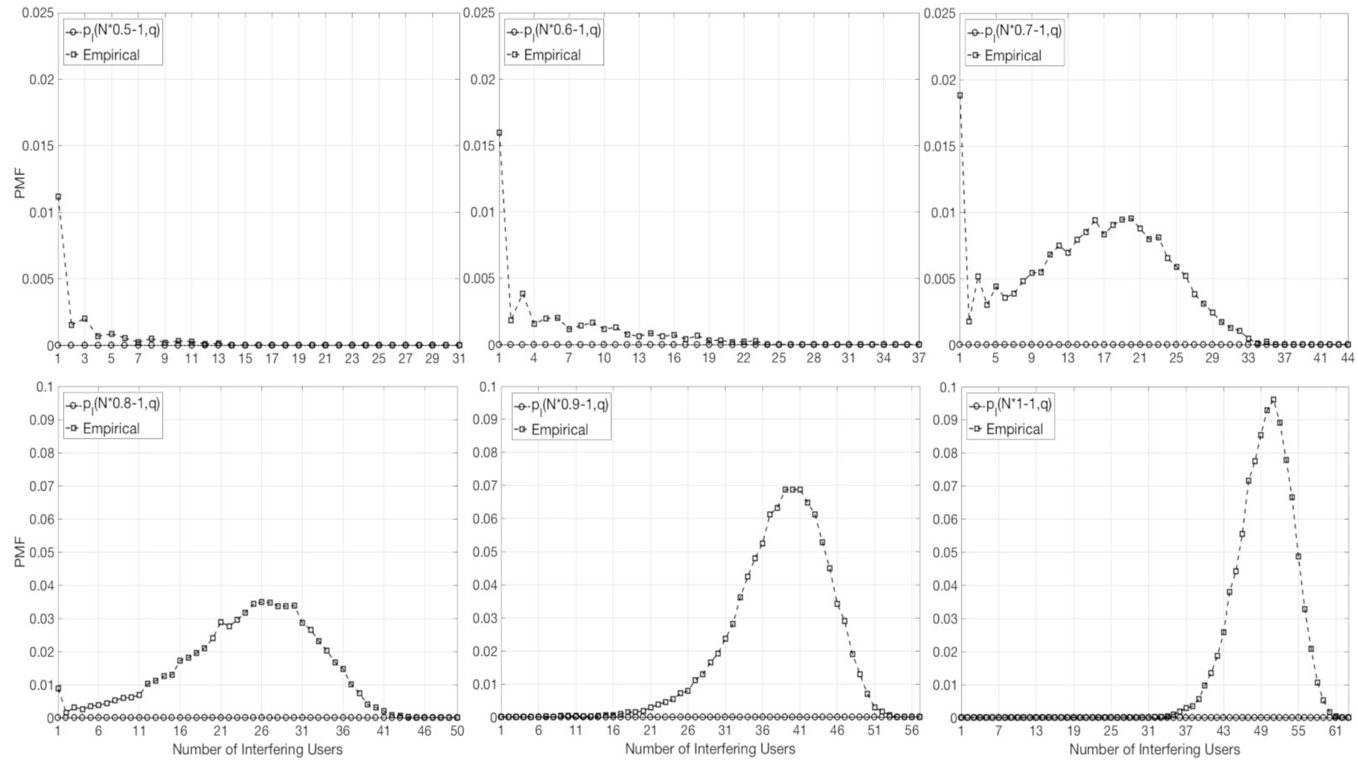

Fig. 3: Empirical distributions of the number of interfering users $l = 1 \cdots 63$ in a loop vs. model in Eq. (1) for $G = 0.5 \cdots 1$. *Empirical* in the legends is $\hat{p}_l$.

TABLE II: Average value of the number of interfering packets $E[I \mid l]$ with a PoI for a loop order l.

	$E[I \mid l]$					
l	*G=0.5*	*G=0.6*	*G=0.7*	*G=0.8*	*G=0.9*	*G=1.0*
1	1	1	1	1	-	-
3	1.10	1.03	1.08	1.04	-	-
5	1.10	1.10	1.14	1.15	-	-
7	1.16	1.19	1.19	1.22	1.32	-
10	1.16	1.22	1.23	1.28	1.48	-
20	-	1.39	1.42	1.47	1.64	-
30	-	-	1.58	1.65	1.83	-
40	-	-	-	1.78	1.94	2.18
50	-	-	-	-	2.00	2.22
60	-	-	-	-	-	2.26

the approximation is even better for $G < 0.5$, but such load values are less significant, since it would mean that the system has been significantly over-provisioned. However, if $G > 0.6$, the model in [11] provides a not negligible error: this is due to the fact that Eq. (1) imposes that $l + 1$ users in a loop share the same K-tuple out of the $\binom{N}{K}$ available ones. The evaluation of a distribution fitting $\hat{p}_l$ will be considered in a future extension of this work. Table II shows the average number of packets $E[I \mid l] = (l+1)K/dim(\mathcal{L}_{l+1})$ interfering with a PoI in a loop of order l over a pool $\mathcal{L}_{l+1} = \{t_1 \cdots t_j\}$ of time slots. Note that l assumes the values in the first column of Table II with probabilities that can be read in the PMFs in Figure 3. In fact, if $l = 1$, the only possible value for the number of interfering packets is 1. Such an event occurs with a probability that decreases with G. For $G > 0.8$, the probability of having $l = 1$ is almost zero [12]. Again, Eq. (1) assumes that $l + 1$ users in a loop draw the same K-tuple in a frame. When this occurs, the number of mutually interfering packets in one of the K time slots is exactly $l + 1$. For the sake of the exemplification, let us consider the case of $G = 1$ with 61 users in a loop: it would mean that $K = 3$ time slots with 61 interfering packets must exist, according to Eq. (1). Contrarily, Table II shows that an average of *only* $2.26+1 = 3.26$ packets are transmitted in each time slot pertaining to the loop, i.e., the pool of time slots in the loop is $(61K)/3.26 \approxeq 56$. In fact, only eight time slots (64-56) are not in the pool of those in loop. It is worth noting that having 3 users (out of 64, i.e., $G = 1$) not in the loop requires 5 to 9 time slots not in the loop, as exemplified in Table III. Finally, Figure 4

TABLE III: Example of the minimum number of time slots ($t_i = 5$) in order to allocate $u_j = 3$ users without loops.

	t_1	t_2	t_3	t_4	t_5
u_1	o			o	o
u_2		o		o	o
u_3			o	o	o

shows the resulting PLR for 3-CRDSA by comparing: (*i*) the simulation results; (*ii*) PLR in Eq. (3); (*iii*) $\widehat{PLR}$ calculated by exploiting Eq. (3) with $\hat{p}_l$ and $\widehat{\zeta_l}$ from Eq. (9). Figure 4 takes into account a range of normalized offered loads around realistic system working points, as identified in [15], [16]. PLR performance depicted in Figure 4 are calculated with the analytical framework proposed in this work, which shows a better fit with the simulation results w.r.t. the approach in Eq.

(3) [11]. It must be noted that obtaining a closed form for $\hat{p}_l$ and $E[I \mid l]$ would offer a complete and accurate modeling of SIC and contention resolution in enhanced F-DSA systems.

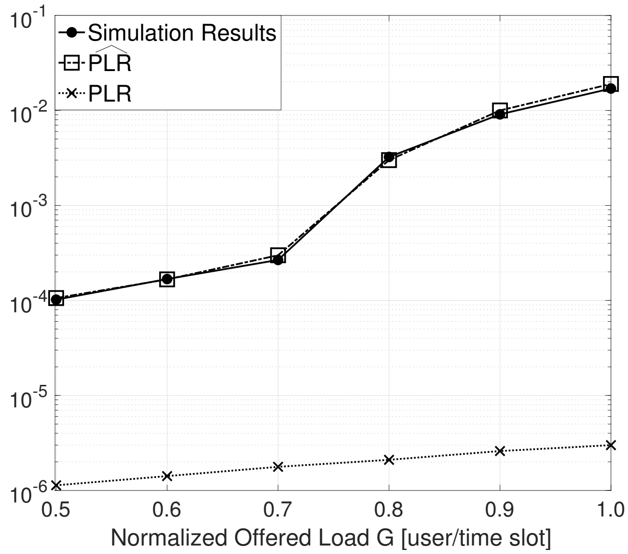

Fig. 4: PLR for 3-CRDSA with Rician fading: simulation results vs. PLR in Eq. (3) vs. our statistical analysis $\widehat{PLR}$.

V. Conclusions

This paper investigated the use of the CRDSA scheme to access the satellite channel in maritime communications. To this end, advanced analytical frameworks and suitable simulation tools have been adopted for carrying out the performance evaluation, by taking as reference the recent scientific works on this subject. Particular attention has been devoted to the mismatch between existing analytical models and simulation results, deriving from the difficulty to correctly estimate the loop probability and the resulting PLR in a D-FSA system. To take these important aspects into consideration, this paper has provided some insights on loop events, the distribution of packets and of users in a loop, and how they can be combined in frames with the presence of loops, eventually proposing a theoretical framework. The performance evaluation shows the good match between the proposed approach and the simulation results.

Acknowledgments

The authors would like to thanks Dr. Marco Colucci for his precious contributions to the simulation campaign.

References

[1] O. D. R. Herrero and R. De Gaudenzi, "High Efficiency Satellite Multiple Access Scheme for Machine-to-Machine Communications," *IEEE Transactions on Aerospace and Electronic Systems*, vol. 48, no. 4, pp. 2961–2989, 2012.

[2] N. Celandroni, E. Ferro, and A. Gotta, "RA and DA satellite access schemes: a survey and some research results and challenges," *International Journal of Communication Systems*, vol. 27, no. 11, pp. 2670–2690, 2014.

[3] N. Celandroni and R. Secchi, "Suitability of DAMA and Contention-Based Satellite Access Schemes for TCP Traffic in Mobile DVB-RCS," *IEEE Transactions on Vehicular Technology*, vol. 58, no. 4, pp. 1836–1845, May 2009.

[4] E. Casini, R. D. Gaudenzi, and O. Herrero, "Contention Resolution Diversity Slotted ALOHA (CRDSA): An Enhanced Random Access Scheme for Satellite Access Packet Networks," *IEEE Transactions on Wireless Communications*, vol. 6, no. 4, pp. 1408–1419, 2007.

[5] G. Liva, "Graph-Based Analysis and Optimization of Contention Resolution Diversity Slotted ALOHA," *IEEE Transactions on Communications*, vol. 59, no. 2, pp. 477–487, February 2011.

[6] C. Stefanovic, E. Paolini, and G. Liva, "Asymptotic Performance of Coded Slotted ALOHA With Multipacket Reception," *IEEE Communications Letters*, vol. 22, no. 1, pp. 105–108, Jan 2018.

[7] C. H. Wei, R. G. Cheng, and S. L. Tsao, "Modeling and Estimation of One-Shot Random Access for Finite-User Multichannel Slotted ALOHA Systems," *IEEE Communications Letters*, vol. 16, no. 8, pp. 1196–1199, August 2012.

[8] J. Hagenauer, F. Dolainsky, E. Lutz, W. Papke, and R. Schweikert, "The Maritime Satellite Communication Channel-Model, Performance of Modulation and Coding," *IEEE Journal on Selected Areas in Communications*, vol. 5, no. 4, pp. 701–707, 1987.

[9] E. Lutz, D. Cygan, M. Dippold, F. Dolainsky, , and W. Papke, "The Land Mobile Satellite Communication Channel-Recording, Statistics, and Channel Model," *IEEE Transaction on Vehicular Technology*, vol. 40, no. 2, pp. 375–386, 1991.

[10] A. R. Miller, R. M. Brown, and E. Vegh, "New derivation for the rough surface reflection coefficient and for distribution of sea-wave elevations," *Microwaves, Optics and Antennas, IEE Proceedings H*, vol. 131, no. 1, pp. 114–116, 1984.

[11] O. del Rio Herrero and R. De Gaudenzi, "Generalized Analytical Framework for the Performance Assessment of Slotted Random Access Protocols," *IEEE Transactions on Wireless Communications*, vol. 13, no. 2, pp. 809–821, 2014.

[12] M. Bacco, P. Cassarà, E. Ferro, and A. Gotta, "Generalized Encoding CRDSA: Maximizing Throughput in Enhanced Random Access Schemes for Satellite," in *International Conference on Personal Satellite Services*. Springer, 2013, pp. 115–122.

[13] A. Mengali, R. De Gaudenzi, and P.-D. Arapoglou, "Enhancing the Physical Layer of Contention Resolution Diversity Slotted ALOHA," *IEEE Trans. Commun*, vol. 65, no. 10, pp. 4295–4308, 2017.

[14] N. Celandroni, F. Davoli, E. Ferro, and A. Gotta, "On Elastic Traffic via Contention Resolution Diversity Slotted Aloha Satellite Access," *International Journal of Communication Systems*, vol. 29, no. 3, pp. 522–534, 2016.

[15] M. Bacco, T. D. Cola, G. Giambene, and A. Gotta, "TCP-based M2M Traffic via Random-Access Satellite links: Throughput Estimation," *IEEE Transactions on Aerospace and Electronic Systems*, pp. 1–1, 2018.

[16] M. Bacco, P. Cassará, M. Colucci, and A. Gotta, "Modeling Reliable M2M/IoT Traffic Over Random Access Satellite Links in Non-Saturated Conditions," *IEEE Journal on Selected Areas in Communications*, vol. 36, no. 5, pp. 1042–1051, May 2018.

[17] F. Baccelli and B. Blaszczyszyn, "Stochastic Geometry and Wireless Networks, Volume I (theory)," *Foundations and Trends in Networking*, vol. 3, no. 3-4, pp. 249–449, 2009.

[18] ——, "Stochastic Geometry and Wireless Networks, Volume II (applications)," *Foundations and Trends in Networking*, vol. 4, no. 1-2, pp. 1–312, 2009.

[19] J. Puttonen, S. Rantanen, F. Laakso, J. Kurjenniemi, K. Aho, and G. Acar, "Satellite model for Network Simulator 3," in *Proceedings of the 7th International ICST Conference on Simulation Tools and Techniques*. ICST (Institute for Computer Sciences, Social-Informatics and Telecommunications Engineering), 2014, pp. 86–91.